Energy exchanges in a nonlinear meta-cell

Camila da Silveira Zanin, Alireza Ture Savadkoohi, Sébastien Baguet, Régis Dufour

▶ **To cite this version:**

Camila da Silveira Zanin, Alireza Ture Savadkoohi, Sébastien Baguet, Régis Dufour. Energy exchanges in a nonlinear meta-cell. DSTA 2021 16th Conference on Dynamical Systems Theory and Applications, Dec 2021, Lodz, Poland. 10.34658/9788366741201 . hal-04235269

HAL Id: hal-04235269
https://hal.science/hal-04235269

Submitted on 10 Oct 2023

HAL is a multi-disciplinary open access archive for the deposit and dissemination of scientific research documents, whether they are published or not. The documents may come from teaching and research institutions in France or abroad, or from public or private research centers.

L'archive ouverte pluridisciplinaire **HAL**, est destinée au dépôt et à la diffusion de documents scientifiques de niveau recherche, publiés ou non, émanant des établissements d'enseignement et de recherche français ou étrangers, des laboratoires publics ou privés.

Energy exchanges in a nonlinear meta-cell

Camila da Silveira Zanin[1,2], Alireza Ture Savadkoohi[1], Sébastien Baguet[2], and Régis Dufour[2]

[1] Univ Lyon, ENTPE, CNRS, LTDS UMR5513, 69518 Vaulx-en-Velin, France
[2] Univ Lyon, INSA Lyon, CNRS, LaMCoS UMR5259, 69621 Villeurbanne, France

Abstract. Energy exchanges between particles of a two degrees of freedom-dof meta-cell are studied. The nondimensionalized equations of the system are presented and then complexified. Only the first harmonics of the system are kept before applying a time multiple scales method. Detection of system dynamics at different time scales leads to the clarification of the slow invariant manifold and characteristic points of the system. Finally, frequency response curves of the system are presented and quasi-analytical responses are confronted with numerical ones obtained by time direct integration.

Keywords: nonlinear restoring force, time multiple scale method, fast/slow dynamics, slow invariant manifold, equilibrium/singular points

1 Introduction

Different types of nonlinear passive absorbers have been developed since it was shown that the bands of working frequencies for such absorbers are larger than the ones for linear absorbers [1]. In the first studies, the nonlinear energy sink (NES) was composed of a cubic nonlinear restoring forcing function [2]. Then, different types of nonlinearities for these systems have been studied and fabricated, such as vibro-impact [3] and piece-wise linear [4] systems, with applications in acoustics and mechanics. The idea of this chapter is to study a mass-in-mass cell where the coupling term between the two masses is a combination of pure cubic and then piece-wise linear functions. The governing equations of considered model looks like a classical two degrees of freedom (dof) system with a general nonlinear coupling term [5]. The inner mass can be used here as NES.
The organization of this paper is as it follows: The system studied and its nondimensionalized equations are presented in Sect. 2. Analytical methods employed in this study are discussed in Sect. 3. System behaviour at different time scales is detected in Sect. 4. Frequency response curves are presented in 5 and numerical results are discussed in Sect. 6. Finally, the paper is concluded in Sect. 7.

2 Studied system and equations

Let us consider the academic model of the non-dimensionalized system which is illustrated in Fig. 1. Its governing equations in the time domain τ reads:

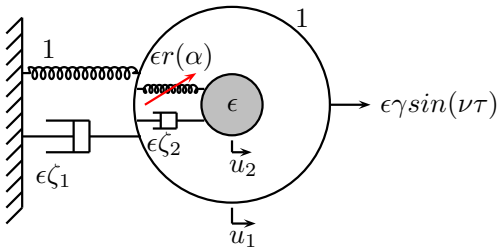

Fig. 1: Model of the nondimensionalized mass-in-mass meta-cell.

.

$$\begin{cases} \ddot{u}_1 + u_1 + \epsilon\zeta_1\dot{u}_1 + \epsilon r(u_1 - u_2) + \epsilon\zeta_2(\dot{u}_1 - \dot{u}_2) = \epsilon\gamma\sin(\nu\tau) \\ \epsilon\ddot{u}_2 + \epsilon r(u_2 - u_1) + \epsilon\zeta_2(\dot{u}_2 - \dot{u}_1) = 0 \end{cases} \tag{1}$$

where $(\dot{\ })$ stands for derivative of a variable with respect to τ. This system can correspond to a mass-in-mass cell with $\frac{m_2}{m_1} = \epsilon \ll 1$, where m_1 and m_2 stand for masses of outer and inner oscillators, respectively.

Both masses are coupled via a damping coefficient and a nonlinear restoring forcing term, $r(\alpha)$, which is function of the relative displacement of the two masses. $r(\alpha)$ combines smooth (cubic) and non-smooth (piece-wise linear) nonlinearities, reading as:

$$r(\alpha) = \begin{cases} k_{NL}\alpha^3 & \text{if } -\delta \leq \alpha \leq \delta \\ k_L(\alpha - \delta) + k_{NL}\delta^3 & \text{if } \alpha > \delta \\ k_L(\alpha + \delta) - k_{NL}\delta^3 & \text{if } \alpha < -\delta \end{cases} \tag{2}$$

In addition, the variables w and v, corresponding to the centre of mass and the relative displacement of two particles, respectively, are introduced as:

$$\begin{cases} w = u_1 + \epsilon u_2 \\ v = u_1 - u_2 \end{cases} \tag{3}$$

Thus, Eq. 1 is re-written in the following form:

$$\begin{cases} \ddot{w} + w + \epsilon v + \epsilon\zeta_1(\dot{w} + \epsilon\dot{v}) = \epsilon\gamma\sin(\nu\tau) \\ \ddot{v} + w + \epsilon v + \epsilon\zeta_1(\dot{w} + \epsilon\dot{v}) + r(v)(\epsilon + 1) + \zeta_2\dot{v}(\epsilon + 1) = \epsilon\gamma\sin(\nu\tau) \end{cases} \tag{4}$$

3 Complexification and multiple time scales method

Here, we will use the complexification method of Manevitch [6]. The following variables are introduced:

$$\begin{cases} \phi_1 e^{i\nu\tau} = \dot{w} + i\nu w \\ \phi_2 e^{i\nu\tau} = \dot{v} + i\nu v \end{cases} \tag{5}$$

with $i^2 = -1$.
In addition, as stated by the multiple time scales method [7], the time is decomposed in fast (τ_0) and slow scales ($\tau_j = \epsilon^j \tau, j = 1, 2, ...$).
In order to keep only the first harmonics of the system, a Galerkin method is used. For a generic function $Y(\phi_1, \phi_2, \phi_1^*, \phi_2^*)$, this task is achieved by:

$$Z(\phi_1, \phi_2, \phi_1^*, \phi_2^*) = \frac{\nu}{2\pi} \int_0^{\frac{2\pi}{\nu}} Y(\phi_1, \phi_2, \phi_1^*, \phi_2^*) e^{-i\nu\tau} d\tau \tag{6}$$

where $(.)^*$ is the complex conjugate of a variable. It is assumed that $\phi_1, \phi_2, \phi_1^*, \phi_2^*$ do not depend on fast timescale, i.e., $\tau_0 = \tau$, which is checked during the multiple scale analysis, or via searching an asymptotic state when $\tau_0 \to \infty$ [8].
Applying Eq. 5 and 6 in system 4, yields:

$$\begin{cases} \frac{1}{2}\dot{\phi}_1 + \frac{i\nu\phi_1}{2} + \frac{\phi_1}{2i\nu} + \epsilon\zeta_1 \left(\frac{\phi_1}{2} + \epsilon\frac{\phi_2}{2} \right) + \epsilon\frac{\phi_2}{2i\nu} - \frac{\epsilon\gamma}{2i} = 0 \\ \\ \frac{1}{2}\dot{\phi}_2 + \frac{i\nu}{2}\phi_2 + \frac{\phi_1}{2i\nu} + \epsilon\frac{\phi_2}{2i\nu} + \epsilon\zeta_1 \left(\frac{\phi_1}{2} + \epsilon\frac{\phi_2}{2} \right) + \mathcal{R}(\phi_2, \phi_2^*)(\epsilon + 1) \\ + \zeta_2 \frac{\phi_2}{2}(\epsilon + 1) - \frac{\epsilon\gamma}{2i} = 0 \end{cases} \tag{7}$$

Where $\mathcal{R}(\phi_2, \phi_2^*)$ is:

$$\mathcal{R}(\phi_2, \phi_2^*) = -\frac{i\phi_2}{2\nu} G(|\phi_2|^2), \tag{8}$$

$G(|\phi_2|^2)$ depends on the relative displacement of the two masses and can be written as:

$$G(|\phi_2|^2) = \begin{cases} \frac{3K_{NL}|\phi_2|^2}{4\nu^3} & \text{if } \frac{|\phi_2|}{\nu} < \delta \\ \\ \frac{3K_{NL}|\phi_2|^2}{4\nu^3} + \frac{1}{4\pi\nu^3|\phi_2|} \Bigg[\left(-8\delta K_L \nu^3 \sqrt{1 - \frac{\delta^2\nu^2}{|\phi_2|^2}} \right) \\ + K_{NL} \left(-6\delta|\phi_2|^2\nu \sqrt{1 - \frac{\delta^2\nu^2}{|\phi_2|^2}} + 12\delta^3\nu^3 \sqrt{1 - \frac{\delta^2\nu^2}{|\phi_2|^2}} \right) \\ + (8K_L|\phi_2|\nu^2 - 6K_{NL}|\phi_2|^3) \arccos\left(\frac{\delta\nu}{|\phi_2|} \right) \Bigg] & \text{if } \frac{|\phi_2|}{\nu} \geq \delta \end{cases} \tag{9}$$

So one can write:

$$G(|\phi_2|^2) = g(|\phi_2|^2) + \mathcal{O}(\epsilon^1) \tag{10}$$

4 Detection of system behaviour at different time scales

In this section, Eq. 7 will be treated in different scales of ϵ, leading to the determination of different system dynamics, i.e., fast and slow ones [9].

4.1 Fast time scale

The first equation of system 7 at $\mathcal{O}(\epsilon^0)$ reads:

$$\frac{\partial \phi_1}{\partial \tau_0} = 0 \Rightarrow \phi_1 = \phi_1(\tau_1, \tau_2, ...) \tag{11}$$

while the second equation at $\mathcal{O}(\epsilon^0)$ reads:

$$\frac{\partial \phi_2}{\partial \tau_0} = H(\phi_1, \phi_2, \phi_1^*, \phi_2^*) \tag{12}$$

with

$$H = -i\phi_2 + i\phi_1 + i\phi_2 g(|\phi_2|^2) - \zeta_2 \phi_2 \tag{13}$$

when we look for an asymptotic state of the system, that is when $\tau_0 \to \infty$ and $\frac{\partial \phi_2}{\partial \tau_0} \to 0$, considering the system behaviours around a 1:1 resonance and setting $\nu = 1 + \sigma\epsilon$, where σ is a detuning parameter. H is called Slow Invariant Manifold (SIM), which is a geometrical curve corresponding to dynamical destinations of the system. Furthermore, looking to Eq. 11 and 13, the hypothesis of applying Eq. 6 is verified.
The complex variables of Manevitch [6] can be written in the polar domain as:

$$\phi_j = N_j e^{i\delta_j} \tag{14}$$

where $N_j \in \mathbb{R}_+$ and $\delta_j \in \mathbb{R}$, $j = 1, 2$.
Then Eq. 13 in real domain reads:

$$N_1 = N_2 \sqrt{(1 - g(N_2^2))^2 + \zeta_2^2} \tag{15}$$

An example of the SIM Considering the parameters of the system presented in Table 1, the SIM, obtained from Eq. 15, is plotted in Fig. 2. The geometry of the SIM exhibits four local extrema, differing from corresponding ones of systems with pure cubic and also with only piecewise-linear nonlinearities, which present two local extrema [10, 11].

Table 1: Parameters of the system.

ζ_1	ζ_2	γ	K_{NL}	K_L	δ
0.1	0.1	0	0.1	0.1	5

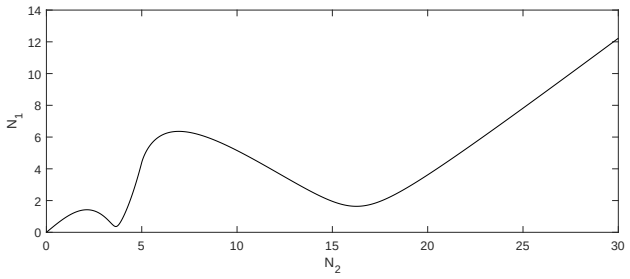

Fig. 2: The SIM of the system with given parameters in Table 1.

4.2 Slow time scale

The first equation of system 7 at $\mathcal{O}(\epsilon^1)$ reads:

$$\frac{\mathrm{d}\phi_1}{\mathrm{d}\tau_1} = E_1(\phi_1, \phi_2, \phi_1^*, \phi_2^*) \tag{16}$$

where

$$E_1(\phi_1, \phi_2, \phi_1^*, \phi_2^*) = -2i\sigma\phi_1 - \zeta_1\phi_1 + i\phi_2 - i\gamma = 0 \tag{17}$$

The evolution of the SIM (see Eq. 13) in τ_1 time scale can be written in matrix form as:

$$\underbrace{\begin{bmatrix} \dfrac{\partial H}{\partial \phi_2} & \dfrac{\partial H}{\partial \phi_2^*} \\ \dfrac{\partial H^*}{\partial \phi_2} & \dfrac{\partial H^*}{\partial \phi_2^*} \end{bmatrix}}_{B} \begin{bmatrix} \dfrac{\partial \phi_2}{\partial \tau_1} \\ \dfrac{\partial \phi_2^*}{\partial \tau_1} \end{bmatrix} = - \begin{bmatrix} \dfrac{\partial H}{\partial \phi_1} & \dfrac{\partial H}{\partial \phi_1^*} \\ \dfrac{\partial H^*}{\partial \phi_1} & \dfrac{\partial H^*}{\partial \phi_1^*} \end{bmatrix} \begin{bmatrix} \dfrac{\partial \phi_1}{\partial \tau_1} \\ \dfrac{\partial \phi_1^*}{\partial \tau_1} \end{bmatrix} \tag{18}$$

Let us seek for singular and equilibrium points, which correspond to non-periodic and periodic regimes, respectively [8]:

Singular points The following conditions are set:

$$\begin{cases} E_1(\phi_1, \phi_2, \phi_1^*, \phi_2^*) = 0 \\ H(\phi_1, \phi_2, \phi_1^*, \phi_2^*) = 0 \\ \det(B) = 0 \end{cases} \tag{19}$$

From $\det(B) = 0$, the position of possible singular points are determined as:

$$1 + g^2(N_2^2) - 2g(N_2^2) - 2N_2^2 g'(N_2^2) + 2N_2^2 g(N_2^2) g'(N_2^2) + \zeta_2^2 = 0 \tag{20}$$

Equilibrium points The following conditions are set:

$$\begin{cases} E_1(\phi_1, \phi_2, \phi_1^*, \phi_2^*) = 0 \\ H(\phi_1, \phi_2, \phi_1^*, \phi_2^*) = 0 \\ \det(B) \neq 0 \end{cases} \tag{21}$$

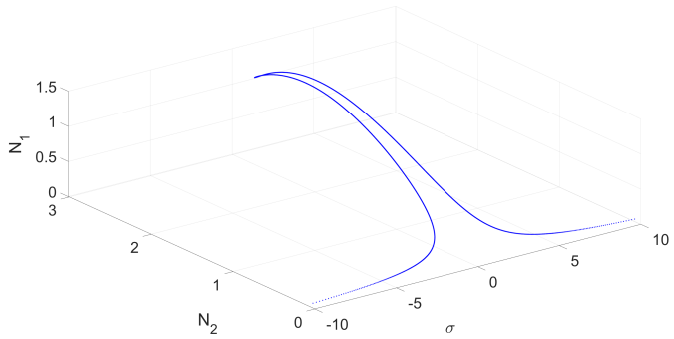

Fig. 3: Possible equilibrium points of the system with respect to the de-tuning parameter σ for the system with $\gamma = 1$. Results are obtained from Eqs. 23 and 15.

From 21, equilibrium points are computed as:

$$\begin{aligned} &N_2^2 g^2(N_2^2)(4\sigma^2 + \zeta_1^2) + N_2^2 g(N_2^2)(-8\sigma^2 + 4\sigma - 2\zeta_1^2) \\ &+N_2^2(\zeta_1^2\zeta_2^2 + 2\zeta_1\zeta_2 + 4\sigma^2 - 4\sigma + 1 + \zeta_1^2 + 4\sigma^2\zeta_2^2) - \gamma^2 = 0 \end{aligned} \tag{22}$$

Solving this equation directly is challenging due to its non-smooth nature. However, this equation can be reorganized with respect to σ parameter, becoming a polynomial of degree two (Eq. 23) which can easily be solved.

$$\begin{aligned} &\left(4N_2^2 g^2(N_2^2) - 8N_2^2 g(N_2^2) + 4N_2^2 + 4N_2^2\zeta_2^2\right)\sigma^2 + \left(4N_2^2 g(N_2^2) - 4N_2^2\right)\sigma \\ &+N_2^2\left(g^2(N_2^2)\zeta_1^2 - 2g(N_2^2)\zeta_1^2 + \zeta_1^2\zeta_2^2 + 2\zeta_1\zeta_2 + 1 + \zeta_1^2\right) - \gamma^2 = 0 \end{aligned} \tag{23}$$

For a given forcing amplitude γ and a given N_2, Eq. 23 can be solved with respect to σ, then the frequency response curve in term of N_2 can be obtained. Subsequently, from Eq. 15, the frequency response curve in term of N_1 can also be obtained.

5 Frequency response curves

In this section, some examples of frequency response curves will be presented. Figure 3 presents the three-dimensional view of frequency responses corresponding to the forcing amplitude $\gamma = 1$. This curve is obtained from Eq. 23. This figure shows the position of all possible equilibrium points with respect to the de-tuning parameter σ for the system with $\gamma = 1$.
Two-dimensional views of Fig. 3 are presented in Figs. 4a, 4b and 4c. Figure 4c is in fact a part of the SIM of the system, showing the position of all possible equilibrium points on the SIM for $\gamma = 1$, as it is highlighted in Fig. 4d.

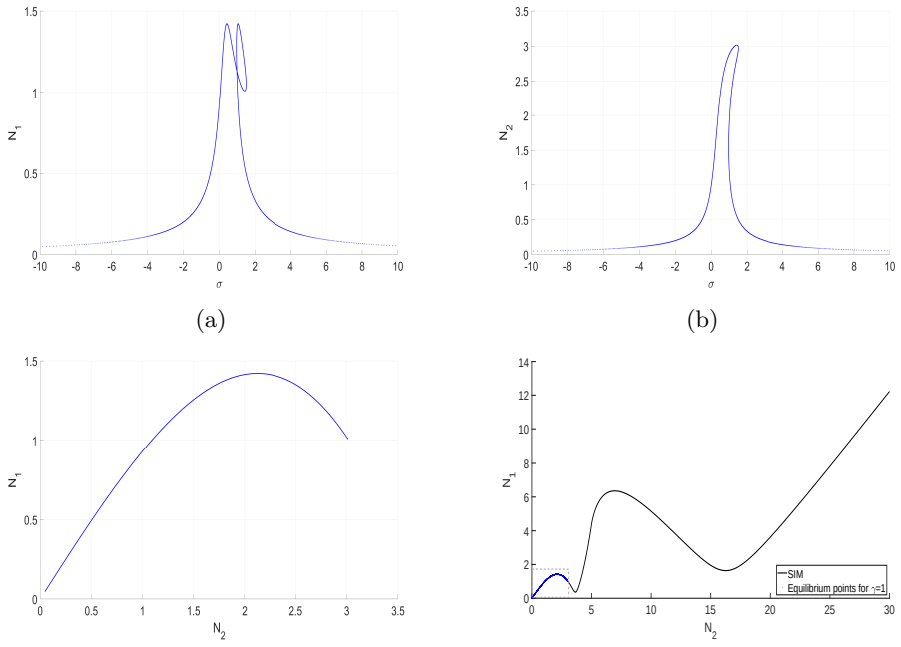

Fig. 4: Two-dimensional views of Fig. 3. a) N_1 with respect to the de-tuning parameter σ; b) N_2 with respect to σ; c) N_1 versus N_2; d) Superposition of Fig. 4c on the SIM of Fig. 2.

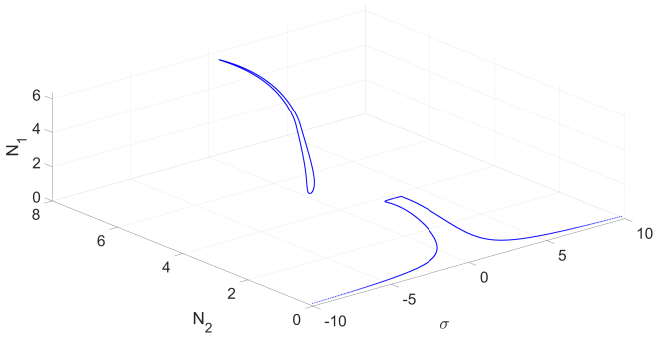

Fig. 5: Possible equilibrium points of the system with respect to the de-tuning parameter σ for the system with $\gamma = 1.5$. Results are obtained from Eqs. 23 and 15.

Figure 5 shows the three-dimensional frequency response curve of the system with the amplitude forcing term $\gamma = 1.5$. It is seen that the system presents an isola, which possesses high energy level for N_1 in comparison to the ones situated in the main part of the frequency responses. Figure 6 presents the two-dimensional views of Fig. 5. From Figs. 6a and 6b, it is seen that, depending on the position of σ, the system can present more than one equilibrium point.

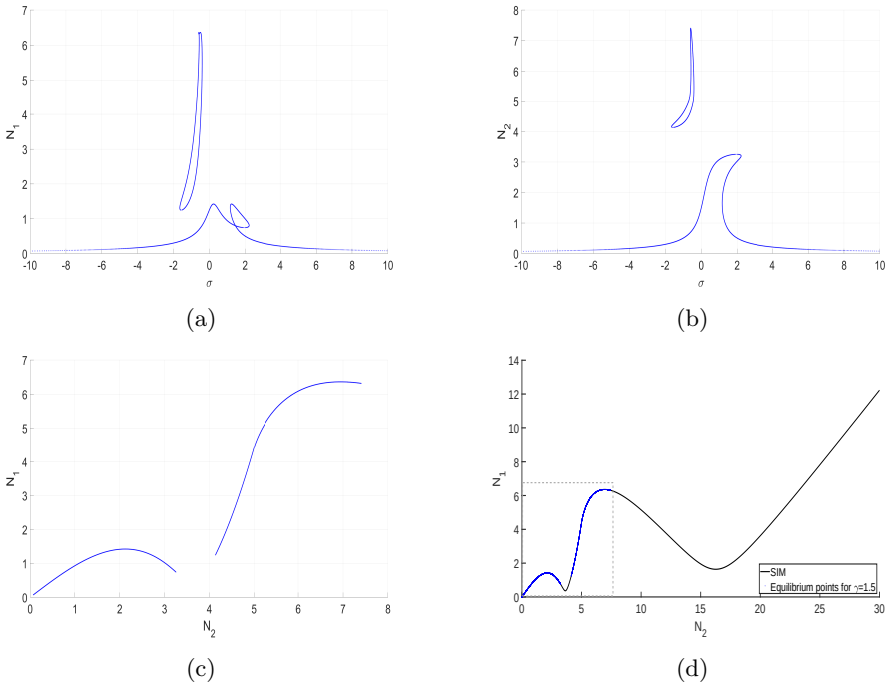

Fig. 6: Two-dimensional views of Fig. 5. a) N_1 with respect to the de-tuning parameter σ; b) N_2 with respect to σ; c) N_1 versus N_2; d) Superposition of Fig. 6c on the SIM of Fig. 2.

6 Numerical responses

In this section, some numerical responses, obtained by direct numerical integration of Eq. 4, will be presented and confronted with quasi-analytical ones.
Figure 7a presents the SIM accompanied by free numerical responses of the system for the initial conditions $(w, v, \dot{w}, \dot{v}) = (7, 7, 0, 0)$. It is seen that, starting from the initial condition, the system follows the SIM and it bifurcates twice before going to the rest position (as expected for free responses). The behaviours

of N_1 and N_2 over time are depicted in Figs. 7b and 7c, respectively.

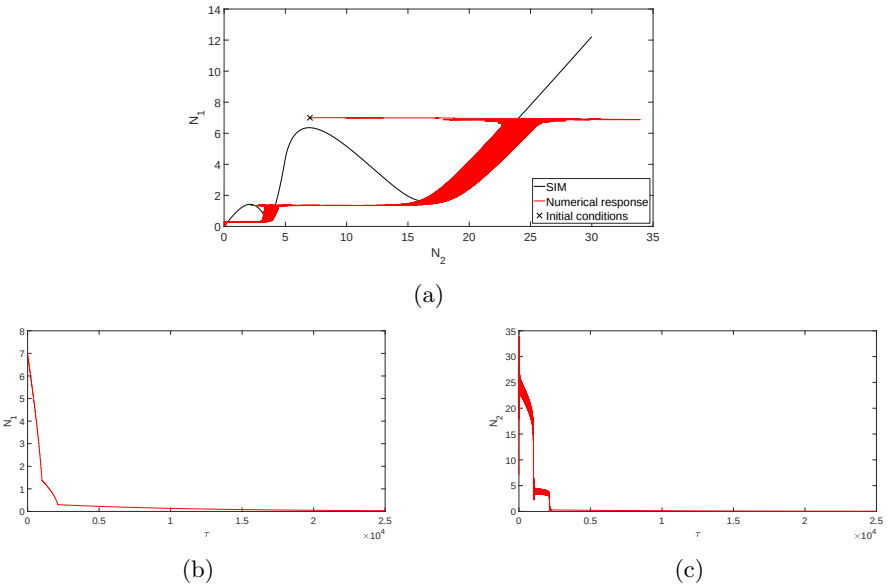

(a)

(b) (c)

Fig. 7: a) The SIM of the system and corresponding numerical responses for $\gamma = 0$ and the initial conditions $(w, v, \dot{w}, \dot{v}) = (7, 7, 0, 0)$; b) N_1 versus τ; c) N_2 versus τ.

Figure 8a presents numerical responses of the system for $\gamma = 1$ and $\sigma = 0$ under the initial conditions $(w, v, \dot{w}, \dot{v}) = (7, 7, 0, 0)$. Comparing Figs. 8b and 8c with Figs. 4a and 4b, respectively, we see that the numerical responses converge to the equilibrium points already predicted by our developments .

7 Conclusion

The studied system can be considered as mass-in-mass cell with a nonlinear compound restoring forcing function, which couples two masses. This system can be used for the control of the outer mass, representing the principal system.
The nondimensionalized equations of the system are complexified, thuncated and treated by the time multiple scale method. Thus, the slow invariant manifold of the system is detected, which presents four local extrema and differs from corresponding ones of system with pure cubic nonlinearities, for example. Singular and equilibrium points are also obtained, leading to the detection of frequency responses of the system, which provides a three-dimensional view of possible equilibrium points for a given forcing ampitude. Finally, quasi-analytical

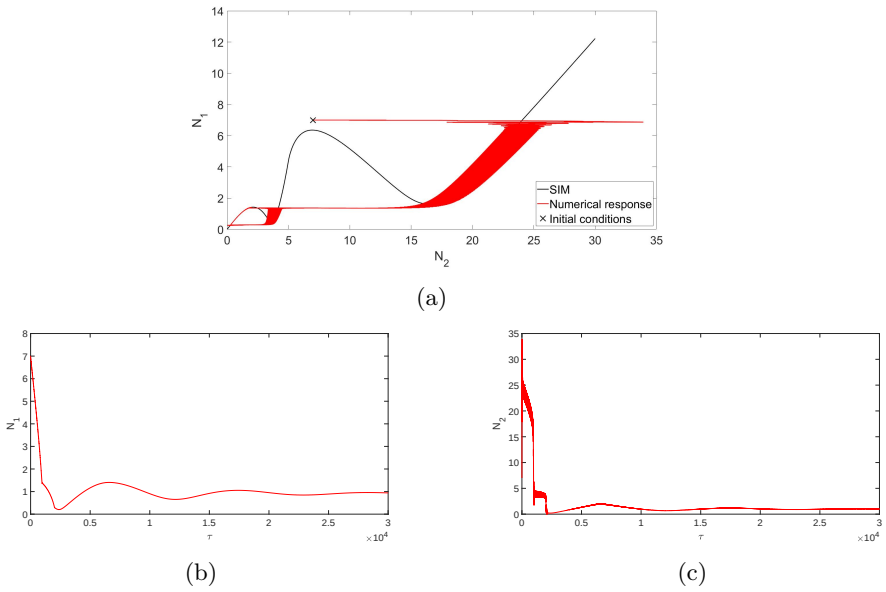

(a) (b) (c)

Fig. 8: The SIM of the system and corresponding numerical responses for $\gamma = 1$, $\sigma = 0$ and the initial conditions $(w, v, \dot{w}, \dot{v}) = (7, 7, 0, 0)$; b) N_1 versus τ; c) N_2 versus τ.

responses are confronted with numerical ones obtained by time direct integration. The developments of this paper provide tools for designing the inner mass for the aim of energy control or localization.

Acknowledgments This work was supported by the LABEX CeLyA (ANR-10-LABX-0060) of Université de Lyon, within the program "Investissements d'Avenir" operated by the French National Research Agency (ANR).

References

1. Roberson, R.E.: Synthesis of a nonlinear dynamic vibration absorber. Journal of the Franklin Institute. 254(3), 205-220 (1952). doi:10.1016/0016-0032(52)90457-2
2. Vakakis, A. F.: Inducing Passive Nonlinear Energy Sinks in Vibrating Systems. J. Vib. Acoust. 123(3), 324-332 (2001). doi:10.1115/1.1368883
3. Gendelman, O.V.: Analytic treatment of a system with a vibro-impact nonlinear energy sink. J. of Sound and Vibration. 331(21), 4599-4608, . 10.1016/j.jsv.2012.05.021
4. Lamarque, C.-H., Gendelman, O.V., Ture Savadkoohi, A. et al. Targeted energy transfer in mechanical systems by means of non-smooth nonlinear energy sink. J. Acta Mech. 221, 175 (2011). doi:10.1007/s00707-011-0492-0

5. Vakakis A. F. Nonlinear targeted energy transfer in mechanical and structural systems. In: Nonlinear Targeted Energy Transfer in Mechanical and Structural Systems (2008)
6. Manevitch, L.I., Waterman, M.S.: The Description of Localized Normal Modes in a Chain of Nonlinear Coupled Oscillators Using Complex Variables. J. Nonlinear Dyn. 25, 95-109 (2001). doi:10.1023/A:1012994430793
7. Nayfeh A., Mook D. I.: Nonlinear Oscillations. John Wiley and Sons, New York (1979).
8. Ture Savadkoohi, A., Lamarque, C.-H., Weiss, M. et al.: Analysis of the 1:1 resonant energy exchanges between coupled oscillators with rheologies. J. Nonlinear Dyn. 86, 2145-2159 (2016). doi:10.1007/s11071-016-2792-3
9. Charlemagne, S., Ture Savadkoohi, A., Lamarque, C.-H.: Interactions Between Two Coupled Nonlinear Forced Systems: Fast/Slow Dynamics. International Journal of Bifurcation and Chaos. 26 (09) (2016). doi:10.1142/S0218127416501558
10. Gendelman, O.V.: Targeted energy transfer in systems with non-polynomial nonlinearity. J. of Sound and Vibration. 315, 732-745 (2008). doi:10.1016/j.jsv.2007.12.024
11. Gendelman, O.V., Starosvetsky, Y., Feldman, M.: Attractors of harmonically forced linear oscillator with attached nonlinear energy sink I: Description of response regimes. J. Nonlinear Dyn. 51, 31-46 (2008). doi:10.1007/s11071-006-9167-0